

# Imaging Flow Cytometry With Femtosecond Laser-Micromachined Glass Microfluidic Channels

Veerendra Kalyan Jagannadh, Mark D. Mackenzie, Parama Pal, Ajoy K. Kar, *Member, IEEE*, and Sai Siva Gorthi, *Member, IEEE*

**Abstract**—Microfluidic/optofluidic microscopy is a versatile modality for imaging and analyzing properties of cells/particles while they are in flow. In this paper, we demonstrate the integration of fused silica microfluidics fabricated using femtosecond laser machining into optofluidic imaging systems. By using glass for the sample stage of our microscope, we have exploited its superior optical quality for imaging and bio-compatibility. By integrating these glass microfluidic devices into a custom-built bright field microscope, we have been able to image red blood cells in flow with high-throughputs and good fidelity. In addition, we also demonstrate imaging as well as detection of fluorescent beads with these microfluidic devices.

**Index Terms**—Ultra-fast laser inscription, microfluidic/optofluidic imaging, high-throughput imaging, glass microfluidics.

## I. INTRODUCTION

**I**MAGING Flow Cytometry (IFC) is a versatile platform that combines the benefits of digital microscopy and flow cytometry. The concept of imaging cells in flow was first proposed in the year 1979 [1], [2] and there have been many recent developments in the field of IFC since then.

Amnis Corp has demonstrated an imaging throughput of 5000 cells per second [3] with the use of time delay integration detector. Of late, the synergistic combination of optics and microfluidics has been used to achieve even higher imaging throughputs as well as multidimensional imaging of cells. Imaging throughputs of upto 20,000 beads per second have been demonstrated by employing micro-optics and microfluidics to simultaneously image multiple fields of view [4]. Microfluidic IFC has also been used as a tool for accurately determining 3D morphology of cells

[5]–[8]. In order to observe cellular organelles in an environment similar to their vasculature, fluorescence imaging of cells in flow through microfluidic channels has been exploited [9].

In most of the previously demonstrated IFC systems [4], [9]–[11], microfluidic devices fabricated in Polydimethylsiloxane (PDMS) have been used for sample handling. For example, microfluidic channels have been used to transport the sample across a linear variable filter to enable hyper-spectral imaging of cells in a single shot [12]. Although PDMS microfluidic devices have been reasonably successful as substrates in laboratory prototypes, it suffers from some significant drawbacks that prevent its use in systems that can be translated to the field. The absorptive (chemical) nature of PDMS presents challenges for imaging systems. For example, PDMS is known to absorb small hydrophobic molecules (fluorescent labels like Nile red [13] and Rhodamine B [14]), both of which are commonly used for staining biological specimen for imaging. From subsequent usage, the absorption of these stains into the microfluidic device would result in fluorescence emission from the PDMS device itself [13]. This leads to deterioration of the imaging quality of the system. Apart from PDMS, other polymer materials like PMMA have also been used in IFC systems [15], [16]. However, PMMA also suffers from similar issues as that of PDMS [17].

The robustness and suitability of PDMS devices for long-term use, especially in field-usable prototypes is questionable [18]. Glass microfluidic devices, on the other hand, are more ideal for handling samples in microfluidics-based imaging systems. Glass is more robust, mechanically stable and possesses superior optical quality as compared to PDMS. In addition, glass is bio-compatible and is not known to exhibit absorption of any organic compounds. Few of the previous demonstrations of IFC [6], [7] employ glass microfluidic devices, however they were fabricated using conventional methods [19]. Conventional fabrication of glass microfluidics is a significantly more complex process than soft-lithography (for PDMS). The advent of femtosecond laser micromachining/ultra-fast laser inscription (ULI) has enabled rapid prototyping of three dimensional glass microfluidic devices [20]. Despite these recent significant advances in femtosecond laser micromachining, the applicability of ULI based glass microfluidic devices to IFC systems has not been investigated upon yet. In this paper, we report our investigations on the usability of femtosecond laser micromachined glass microfluidic devices in optofluidic imaging systems. Using ULI processes, we have fabricated glass microfluidic devices consisting of subsurface channels, obviating the need for an additional

Manuscript received October 6, 2014; revised November 16, 2014; accepted December 9, 2014. Date of publication December 18, 2014; date of current version February 27, 2015. This work was supported in part by the UKIERI Project Femtosecond Laser-Micromachined Microfluidics, Integrated Surface Enhanced Raman Scattering Sensors for Point-of-Care Diagnostics. The work of M. D. Mackenzie was supported by EPSRC under Grant EP/J500227/1. The work of V. K. Jagannadh and S. S. Gorthi was supported in part by the Biotechnology Ignition Grant of BIRAC.

V. K. Jagannadh and S. S. Gorthi are with the Department of Instrumentation and Applied Physics, Indian Institute of Science, Bangalore 560012, India (e-mail: veerendra77@iap.iisc.ernet.in; saisiva.gorthi@iap.iisc.ernet.in).

M. D. Mackenzie and A. K. Kar are with the Institute of Photonics and Quantum Sciences, School of Engineering and Physical Sciences, Heriot Watt University, Edinburgh EH14 4AS, U.K. (e-mail: mdm13@hw.ac.uk; A.K.Kar@hw.ac.uk).

P. Pal is with the Robert Bosch Centre for Cyber Physical Systems, Indian Institute of Science, Bangalore 560012, India (e-mail: parama.pal@rbceps.org).

Color versions of one or more of the figures in this paper are available online at <http://ieeexplore.ieee.org>.

Digital Object Identifier 10.1109/JSTQE.2014.2382978

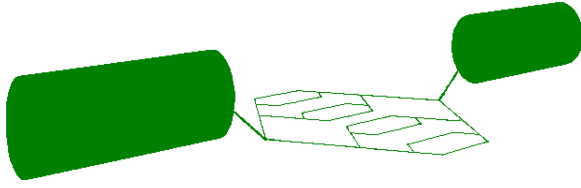


Fig. 1. Schematic of the device fabricated using Laser Inscription. The solid green cylinders denote the inlet and outlet channels of the device.

component to cover the channels. Multiple channels have been used to enable degeneracy as well as to obtain higher imaging throughputs. In the subsequent sections, we outline the process used to fabricate the microfluidic devices and also, demonstrate the usability of these devices in bright-field and fluorescence microfluidic microscopy imaging modalities.

## II. FEMTOSECOND LASER FABRICATION OF MICROFLUIDIC DEVICES

The ULI technique uses ultrashort pulses from a laser to locally modify materials such as fused silica. The sample is transparent to the laser wavelength but absorbs through a multiphoton process when the light is focused onto it. Depending on parameters such as pulse energy, repetition rate and translation speed, several classes of material modifications are possible. The first is a refractive index modification in the material which is useful for fabricating waveguides. The second is the formation of nano-gratings which enables selective chemical etching. Third is the formation of voids in the material. The sample is mounted on a high-precision translation stage and femtosecond pulses are focused onto it using a microscope objective. The sample is moved relative to the incoming focused laser beam in  $x$ ,  $y$  and  $z$  directions to create 3D structures. ULI offers fabrication of 3D devices with much greater ease as compared to other methods of fabricating 3D microfluidic devices such as multi-layer soft-lithography using PDMS [21]. In general, for the case of PDMS, different layers of PDMS have to be fabricated and stacked together to achieve a 3D structure. Whereas, in the case of ULI, 3D structures can be fabricated in a single step. Also fused silica has higher damage thresholds as compared to PDMS and as previously noted, is compatible with many different biological samples and chemicals. ULI is an ideal rapid prototyping technique as it does not require a mask to be created for each modification.

The microfluidic devices used in these experiments were fabricated using ULI and subsequent hydrofluoric acid (HF) etching in fused silica. The device used in these experiments consist of a series of parallel horizontal channels, as shown in Fig. 1, with a width  $\sim 20.7 \mu\text{m}$  and depth of  $\sim 20 \mu\text{m}$ . The design ensures that the cells in each channel are at the correct plane of focus for the microscope and prevents multiple cells from being present in the same channel position at once. As opposed to the PDMS devices used in the known IFC systems, the devices used in these experiments are 3D in nature. The inlet and outlet of the device are offset vertically from the central channels and connected by angled channels to move the imaging

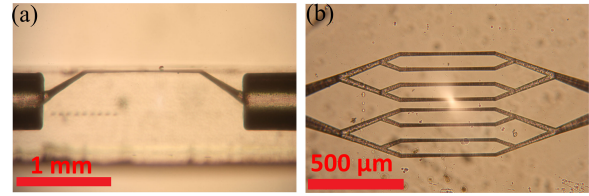


Fig. 2. Device after etching. (a) Side view of the device showing the channel moving up to the surface for imaging. (b) Top view showing the individual channels.

region closer to the surface of the device in accordance with the working distances of the imaging objectives that are commonly available. Using microscopy, it was estimated that the channels were at a depth of around  $60 \mu\text{m}$  from the surface of the glass substrate, which falls well within the working distances of most commonly available objectives. Multiple channels were used in order to simultaneously image cells flowing across different channels and thereby obtain an optimally high throughput. All the channels are simultaneously imaged only at the central region so as to strike an optimal balance between frame rate of acquisition and field of view of the camera. A Fianium HE-1060-1J femtosecond laser set to a repetition rate of 500 kHz, pulse length of 330 fs and power of 250 mW was focused onto the samples mounted on an Aerotech XYZ stage, through a 0.4 NA objective. After writing samples was completed, the samples were etched for approximately 20 hours in 5% HF. Tubing from Upchurch Scientific (outer and inner diameter of  $360 \mu\text{m}$  and  $100 \mu\text{m}$  respectively) was bonded to the inlets using UV curing glue (Thorlabs MIL-A-3920). Fig. 2 shows microscopic images of the microfluidic device after etching.

## III. CHARACTERIZATION OF LASER FABRICATED GLASS MICROFLUIDIC DEVICES FOR IMAGING APPLICATIONS

### A. Experimental Setup

After fabrication, the glass microfluidic devices were tested by imaging different microscopic specimens in flow. In this section, we outline the basic layout of the microfluidics-based high-throughput imaging system used. The schematic of the microfluidics-based imaging flow cytometer is shown in Fig. 3. A high power blue LED (Thorlabs M455L3) was used to uniformly illuminate the sample plane. The image of the LED was focused onto an Iris with an aspheric condenser lens, a second condenser lens was placed at a focal length distance from this iris in a standard Köhler illumination configuration to obtain uniform illumination at the sample plane. The lenses  $L_1$  (Focal length = 20 mm, Diameter = 25.4 mm),  $L_2$  (Focal length = 20 mm, Diameter = 25.4 mm) serve as the collector and condenser lenses of a typical microscope, and the two irises ( $I_1$ ,  $I_2$ ) act as field and condenser diaphragms, respectively. A microfluidic device was placed in the sample plane of the imaging system. For fluorescence imaging, excitation (center wavelength = 475 nm, bandwidth = 35 nm) and emission (center wavelength = 530 nm, bandwidth = 43 nm) filters were used in

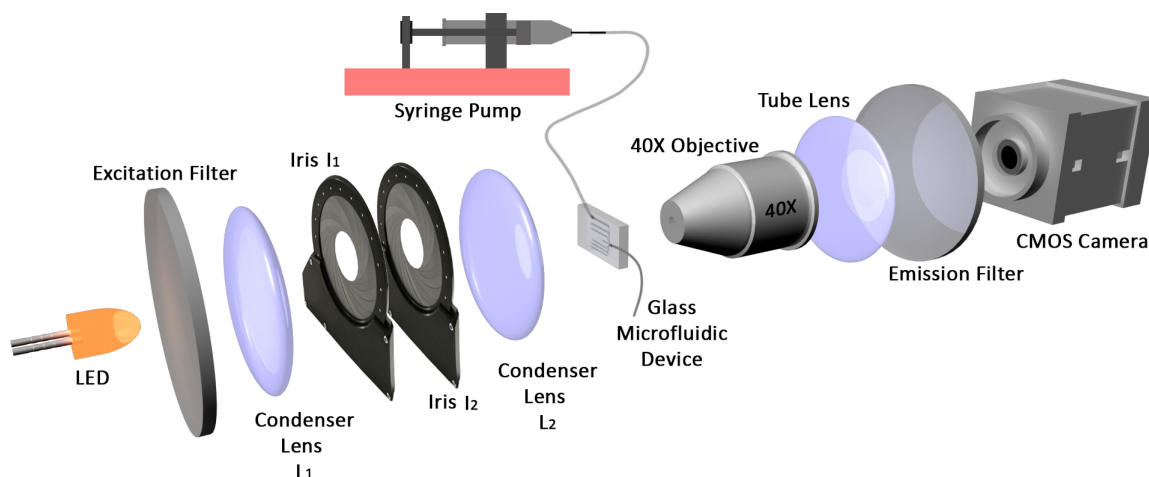


Fig. 3. Schematic of the imaging system used to characterize the femtosecond laser micromachined glass microfluidic devices.

the system and are not needed while performing bright-field imaging.

A microscope objective (40X, NA = 0.75) was used to image the sample plane onto the high-speed Complementary metal-oxide semiconductor camera (Mikrotron eosens MC1362) through a tube lens. The field of view of the imaging system was characterized using a 1951 USAF resolution target and was found to be  $350 \mu\text{m} \times 280 \mu\text{m}$ .

### B. Bright Field Brightfield Imaging Flow Cytometry

Using a syringe pump, a suspension of red blood cells (RBCs) was flown through the glass microfluidic devices at a flow rate of  $400 \mu\text{Lh}^{-1}$ . The instrumentation (without the fluorescence filters) described in the previous section was used to record videos of the flow stream containing RBCs. The videos were recorded at 2550 fps with the exposure set to  $10 \mu\text{s}$ . The recorded videos were post processed to extract the images of different cells. We have used background subtraction to retrieve the images of cells from the videos. A frame not containing any cells was defined as the background and is subtracted from all the frames present in the video. The effect of background subtraction on a given frame is shown in Fig. 4. The background subtracted frames are converted into binary images with appropriate thresholding. The threshold was chosen so that all the portions (pixels) of the image apart from the boundaries of cell(s) were converted to zeros. Following which, different morphological operations were performed to obtain a binary image with all portions inside and on the cell converted to ones. On the thresholded image, connected component analysis was performed using the regionprops function in MATLAB (R2013b, Mathworks Inc.). The centroid of the cell was obtained and subsequently the portion of the frame containing the cell was cropped. In this experiment a total of about 7576 cells were imaged in a duration of 1.6 seconds. The throughput of the system is approximately 4735 cells per second. The representative images of the cells obtained by processing frames in a recorded video of the flow stream have been shown in the Fig. 5. The throughput achieved is comparable to previously demonstrated throughputs in literature [4], [22]. As the basic processing steps are not complex, it does not

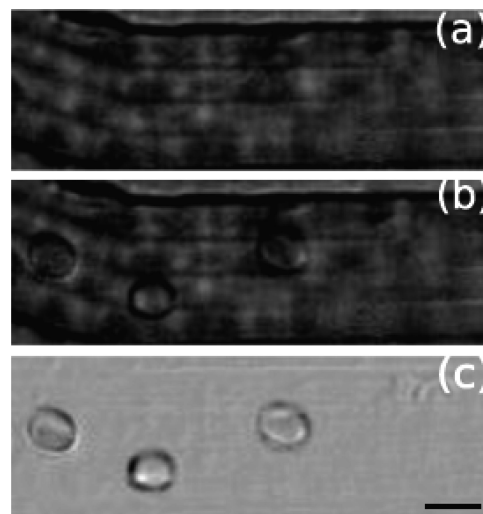


Fig. 4. (a) Background image not containing any cells. (b) Frame containing cells before background subtraction. (c) Frame containing cells after background subtraction. Length of scale bar is  $10 \mu\text{m}$ .

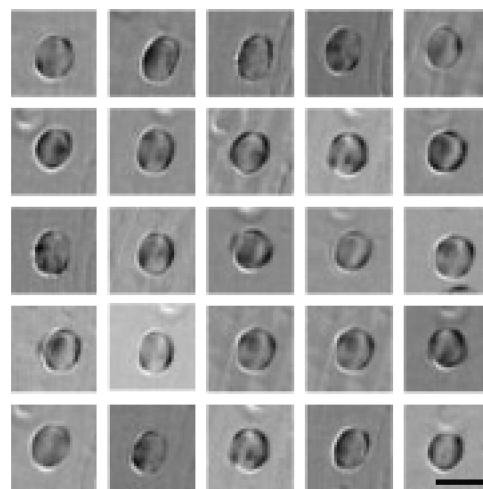


Fig. 5. Representative images of RBCs captured, while they were flowing through the femtosecond laser micromachined microfluidic devices. Length of scale bar is  $10 \mu\text{m}$ .

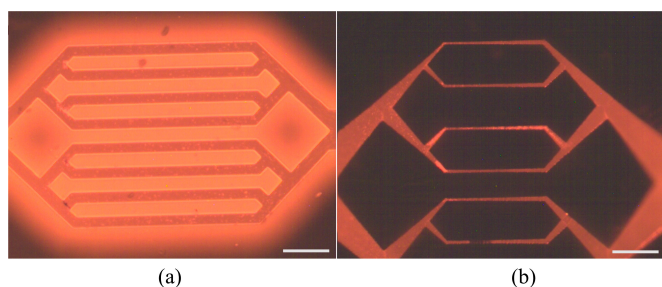


Fig. 6. Chemical absorption of Rhodamine B in PDMS and ULI based glass microfluidic devices. Images of the PDMS and ULI based glass microfluidic devices after Rhodamine B is flown through them for 20 minutes at a flow rate of  $60 \mu Lh^{-1}$  (a) Image of the PDMS microfluidic device (b) Image of the ULI based glass microfluidic device. Length of scale bar is  $500 \mu m$ .

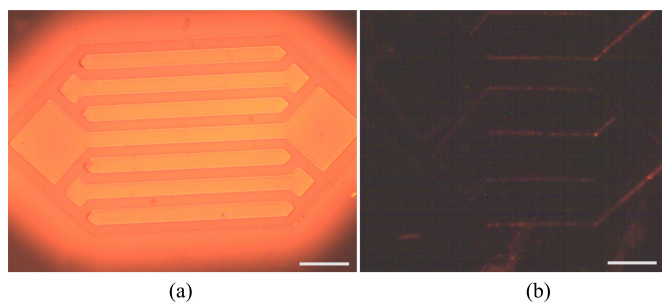


Fig. 7. Images of the PDMS and ULI based glass microfluidic devices after water is flown through the devices so as to remove Rhodamine B (a) Image of the PDMS microfluidic device (b) Image of the ULI based glass microfluidic device. Length of scale bar is  $500 \mu m$

take more than a few minutes to estimate the cell count and also to extract the images of different cells for morphological inspection in a given sample. Blood cell counting is the most commonly performed laboratory diagnostic test. We believe that with the use of these glass microfluidic devices, it is possible to develop inexpensive imaging flow cytometers with potential applications in clinical diagnostics.

### C. Characterization of Chemical Absorption of Fluorescent Molecules

The chemical absorption properties of the presented ULI based microfluidic devices has been characterized and compared with PDMS. A solution of Rhodamine B was flown through both PDMS and glass microfluidic devices at flow rate of  $60 \mu Lh^{-1}$  for a few minutes. Following which, both the devices were imaged under a fluorescence microscope (Olympus IX15) and the recorded images are shown in Fig. 6. As one can clearly observe, the fluorescence emission in the case of ULI based glass device is very well restricted to the channel region; whereas in the case of PDMS, significant fluorescence emission is observed also from regions other than the microfluidic channel. Following which, water was pumped through both the devices so as to wash out the fluorescent dye from channels. From the images of the devices shown in Fig. 7, taken after removal of the dye, the robustness of the ULI based glass microfluidic device is clear from the fact that minimal fluorescence emission has been observed. Whereas, the PDMS device continued to emit

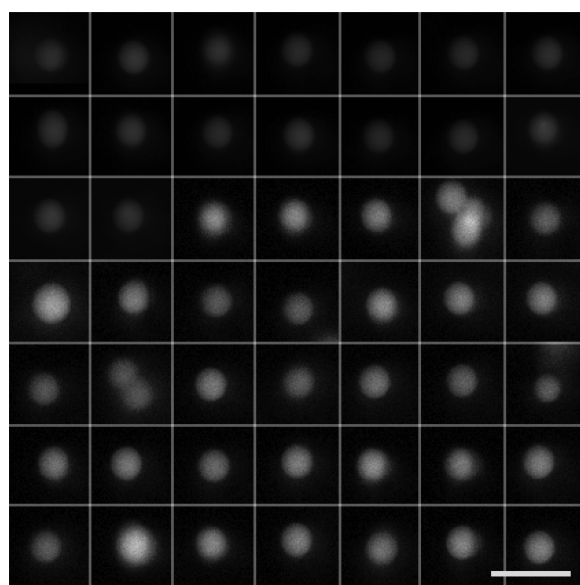


Fig. 8. Representative images of fluorescent microspheres captured, while they were flowing through the femtosecond laser micromachined microfluidic devices. Length of scale bar is  $10 \mu m$ .

fluorescence from regions inside the channels and also regions surrounding them.

### D. Fluorescence Fluorescence Imaging Flow Cytometry

The experimental setup shown in Fig. 3 was used to perform the fluorescence imaging experiments. A suspension of fluorescent beads (Invitrogen F8859, Size =  $4 \mu m$ ) was flown through the microfluidic devices at flow rate of  $20 \mu Lh^{-1}$ . A charge coupled device camera (Pike F-032B) was used in these experiments. The exposure time of the camera was set to  $100 \mu s$  and frame rate was set to 208 fps. The representative images of beads acquired while they were flowing through microfluidic devices are shown in Fig. 8. Higher flow rates ( $90 \mu Lh^{-1}$ ) were used to perform fluorescence detection in the devices. Higher flow rates were used to ensure more particles in the field of view and thereby higher possible fluorescence detection throughputs. As the flow velocity of the particles was high, motion-blur was observed. However, for the case of detection (presence/absence) of the fluorescent bead, motion-blur does not introduce a significant impediment. We have been able to detect approximately 782 beads per second. In the case of fluorescence imaging, computational post-processing steps (like background subtraction), were not required to obtain high fidelity images. In addition, the channel surface imperfections had no effect on the fidelity of the acquired images. The ability to perform fluorescence imaging and detection enables a wide range of medical and biological applications. These microfluidic devices can be used for performing immunofluorescence experiments on individual cells. Immunofluorescence experiments can reveal the distribution of different kinds of proteins and other target molecules across an individual cell. Target-specific fluorescence probes can be used to detect different types of cancers or the presence of bacterial pathogens in a given sample.

## IV. CONCLUSION

IFC is an emerging field with a wide range of applications in microbiology and cellular diagnostics. In this work, we have demonstrated the applicability of femtosecond laser micromachined microfluidic devices for IFC systems. With minimal computational post-processing, we have obtained images of cells and fluorescent beads flowing through these microfluidic devices. By integrating these microfluidic devices into a custom-built bench-top microscope, we have demonstrated high imaging throughputs of about 4735 cells per second.

To the best of our knowledge, the work presented here is the first investigative report on the applicability of ULI based glass microfluidic devices for both bright-field and fluorescence IFC systems. As the outcome of our study is positive, we are hopeful that in future, there would be many demonstrations of ULI based glass microfluidic devices for IFC systems. We believe that our investigations would serve as a guideline to researchers, who intend to employ ULI based glass microfluidic devices for applications in IFC. Glass microfluidic devices present a more robust alternative to PDMS microfluidic devices in end-user prototypes. While PDMS is known to be susceptible to ingress of certain organic solvents resulting in swelling [13], glass does not absorb any organic solvents and hence can be cleaned using any organic solvent for multiple re-usage. This is a significant attribute for on-field deployment of imaging flow cytometers as inexpensive diagnostic instruments.

## REFERENCES

- [1] D. B. Kay, J. L. Cambier, and L. L. Wheeler, "Imaging in flow," *J. Histochem. Cytochem.*, vol. 27, no. 1, pp. 329–334, Jan. 1979.
- [2] V. Kachel, G. Benker, K. Lichtnau, G. Valet, and E. Glossner, "Fast imaging in flow: A means of combining flow-cytometry and image analysis," *J. Histochem. Cytochem.*, vol. 27, no. 1, pp. 335–341, Jan. 1979.
- [3] D. A. Basiji, W. E. Ortyl, L. Liang, V. Venkatachalam, and P. Morrissey, "Cellular image analysis and imaging by flow cytometry," *Clinics Lab. Med.*, vol. 27, no. 3, pp. 653–670, Sep. 2007.
- [4] E. Schonbrun, S. S. Gorthi, and D. Schaak, "Microfabricated multiple field of view imaging flow cytometry," *Lab Chip*, vol. 12, no. 2, pp. 268–273, Dec. 2011.
- [5] S. S. Gorthi and E. Schonbrun, "Phase imaging flow cytometry using a focus-stack collecting microscope," *Opt. Lett.*, vol. 37, no. 4, pp. 707–709, Feb. 2012.
- [6] N. C. Pgard and J. W. Fleischer, "Three-dimensional deconvolution microfluidic microscopy using a tilted channel," *J. Biomed. Opt.*, vol. 18, no. 4, pp. 40 503–40 503, 2013.
- [7] J. Wu, J. Li, and R. K. Y. Chan, "A light sheet based high throughput 3d-imaging flow cytometer for phytoplankton analysis," *Opt. Exp.*, vol. 21, no. 12, pp. 14 474–14 480, Jun. 2013.
- [8] Y. Sung *et al.*, "Three-dimensional holographic refractive-index measurement of continuously flowing cells in a microfluidic channel," *Phys. Rev. Appl.*, vol. 1, no. 1, pp. 014002-1–014002-8, Feb. 2014.
- [9] S. S. Gorthi, D. Schaak, and E. Schonbrun, "Fluorescence imaging of flowing cells using a temporally coded excitation," *Opt. Exp.*, vol. 21, no. 4, pp. 5164–5170, Feb. 2013.
- [10] H. Kim *et al.*, "Development of on-chip multi-imaging flow cytometry for identification of imaging biomarkers of clustered circulating tumor cells," *PLoS ONE*, vol. 9, no. 8, p. e104372, Aug. 2014.
- [11] A. Hattori *et al.*, "Identification of cells using morphological information of bright field/fluorescent multi-imaging flow cytometer images," *Jpn. J. Appl. Phys.*, vol. 53, no. 6S, pp. 06JL03-1–06JL03-4, Jun. 2014.
- [12] G. Di Caprio, D. Schaak, and E. Schonbrun, "Hyperspectral fluorescence microfluidic (HFM) microscopy," *Biomed. Opt. Exp.*, vol. 4, no. 8, pp. 1486–1493, Aug. 2013.
- [13] M. W. Toepke and D. J. Beebe, "PDMS absorption of small molecules and consequences in microfluidic applications," *Lab Chip*, vol. 6, no. 12, pp. 1484–1486, Nov. 2006.
- [14] G. T. Roman, T. Hlaus, K. J. Bass, T. G. Seelhammer, and C. T. Culbertson, "Solgel modified poly(dimethylsiloxane) microfluidic devices with high electroosmotic mobilities and hydrophilic channel wall characteristics," *Anal. Chem.*, vol. 77, no. 5, pp. 1414–1422, Mar. 2005.
- [15] M. Hayashi *et al.*, "Fully automated on-chip imaging flow cytometry system with disposable contamination-free plastic re-cultivation chip," *Int. J. Molecular Sci.*, vol. 12, no. 6, pp. 3618–3634, Jun. 2011.
- [16] K. Yasuda *et al.*, "Non-destructive on-chip imaging flow cell-sorting system for on-chip cellomics," *Microfluidics Nanofluidics*, vol. 14, no. 6, pp. 907–931, Jun. 2013.
- [17] R. Mukhopadhyay, "When PDMS isn't the best," *Anal. Chem.*, vol. 79, no. 9, pp. 3248–3253, May 2007.
- [18] E. K. Sackmann, A. L. Fulton, and D. J. Beebe, "The present and future role of microfluidics in biomedical research," *Nature*, vol. 507, no. 7491, pp. 181–189, Mar. 2014.
- [19] C. Iliescu, H. Taylor, M. Avram, J. Miao, and S. Franssila, "A practical guide for the fabrication of microfluidic devices using glass and silicon," *Biomicrofluidics*, vol. 6, no. 1, pp. 016 505-1–016 505-16, Mar. 2012.
- [20] D. Choudhury, J. R. Macdonald, and A. K. Kar, "Ultrafast laser inscription: Perspectives on future integrated applications," *Laser Photon. Rev.*, vol. 8, pp. 827–846, May 2014.
- [21] M. A. Unger, H.-P. Chou, T. Thorsen, A. Scherer, and S. R. Quake, "Monolithic microfabricated valves and pumps by multilayer soft lithography," *Science*, vol. 288, no. 5463, pp. 113–116, Apr. 2000.
- [22] Amnis imaging flow cytometers. (2014). [Online]. Available: <https://www.amnis.com/imagestream.html>

**Veerendra Kalyan Jagannadh** received the B.E. (Hons.) degree in electronics and instrumentation from the Birla Institute of Technology and Science, Pilani, India, in 2012. He is working toward the Ph.D. degree focusing on development of optofluidics-based biomedical instrumentation for use at the point-of-care. He is currently a Graduate Student at the Indian Institute of Science, Bangalore, India. His research interests include optofluidic imaging techniques and computational imaging flow cytometry.



**Mark D. Mackenzie** received the B.Sc. (Hons.) degree in physics from Edinburgh University, Edinburgh, U.K., in 2011, and the M.Sc. degree in photonics and optoelectronic devices from Heriot-Watt University, Edinburgh, and St. Andrews University, St. Andrews, U.K., in 2012. He is currently working toward the Ph.D. degree focusing on creating a protein-based cell laser (using HEK cells containing GFP) and microfluidic devices (produced by ultrafast laser inscription and hydrofluoric acid etching).



**Parama Pal** received the M.Sc. degree in physics from the Indian Institute of Technology, New Delhi, India, in 2004, and the Ph.D. degree in optics from the Institute of Optics, University of Rochester, Rochester, NY, USA, in 2009. Her thesis was centered on the design and fabrication of postprocessed optical fibers and their subsequent applications for laser systems and microphotonic components. From 2009–2012, she was a Research Fellow at the Wellman Center for Photomedicine, Massachusetts General Hospital, Boston, MA, USA, and the Harvard Medical School, Boston. She is currently the Head of health-care at the Robert Bosch Centre for CyberPhysical Systems, Indian Institute of Science, Bengaluru, India. She received the 'Innovation in Science Pursuit for Inspired Research (INSPIRE)' Faculty Fellowship Award from the Department of Science and Technology (DST) in 2012.



**Ajoy K. Kar** (M'96) received the M.Sc. degree from the Indian Institute of Technology, Delhi, India. He received the Ph.D. degree from the University of Essex, Colchester, U.K., during which he developed his interest in lasers and nonlinear optics. He joined Heriot-Watt University, Edinburgh, U.K., in 1979, where he is currently a Professor at the Institute of Photonics and Quantum Sciences. He has more than 30 years of experience in the investigation of nonlinear optical properties of materials and their applications. He has also pioneered the photonics education in Europe. Some of his current projects include ultrafast laser inscription (ULI) of photonic devices for a broad spectral range from visible to mid-IR and the development of microfluidic devices for biophotonics applications. He is a Founding Member of Optoscribe, a spin-out company specialized in ULI-based photonic device fabrication. He is a Member of the Optical Society of America.



**Sai Siva Gorthi** (M'13) received the Doctorate degree in optical metrology from the Swiss Federal Institute of Technology, Lausanne, Switzerland, in 2010. He is working as an Assistant Professor in the Department of Instrumentation and Applied Physics, Indian Institute of Science (IISc), Bangalore, India. Prior to joining IISc, he was a Postdoctoral Fellow of the Rowland Institute at Harvard University, where he had developed multiple imaging modalities for recording information of fast flowing cells in microfluidic devices. Currently at IISc, part of his group is focusing on the development of various point-of-care diagnostic devices with the combination of optics, microfluidics and electronics. His research interests include imaging flow cytometry, microfluidics and droplet-microfluidics instrumentation, optical metrology. He is Recipient of BIRAC's Biotechnology Ignition Grant Innovator Award in 2014, and DBT's Innovative Young Biotechnologist Award 2013.